

TITLE: CRITICAL PULSE POWER COMPONENTS

MASTER

AUTHOR(S): W. J. Sarjeant and G. J. Rohwein

SUBMITTED TO: 1981 16th Intersociety Energy Conversion
Engineering Conference
Atlanta, Georgia
August 9-14, 1981
(INVITED PAPER)

DISCLAIMER

By acceptance of this article, the publisher recognizes that the U.S. Government retains a nonexclusive, royalty-free license to publish or reproduce the published form of this contribution, or to allow others to do so, for U.S. Government purposes.

The Los Alamos Scientific Laboratory requests that the publisher identify this article as work performed under the auspices of the U.S. Department of Energy.

University of California



LOS ALAMOS SCIENTIFIC LABORATORY

Post Office Box 1663 Los Alamos, New Mexico 87545

An Affirmative Action/Equal Opportunity Employer

CRITICAL PULSE POWER COMPONENTS

W. J. Sarjeant
Los Alamos National Laboratory
Los Alamos, NM 87545

and

G. J. Rohwein
Sandia National Laboratories
Albuquerque, NM 87185

ABSTRACT

Critical components for pulsed power conditioning systems will be reviewed. Particular emphasis will be placed on those components requiring significant development efforts. Capacitors, for example, are one of the weakest elements in high-power pulsed systems, especially when operation at high-repetition frequencies for extended periods of time are necessary. Switches are by far the weakest active components of pulse power systems. In particular, opening switches are essentially nonexistent for most applications. Insulation in all systems and components requires development and improvement. Efforts under way in technology base development of pulse power components will be discussed.

INTRODUCTION

The development of repetitive-operation, long-life, fast-discharge components is essential to many future high-energy applications including nonnuclear or directed energy weapons, isotope separation lasers, short-pulse radar modulators, and electronic warfare and countermeasure pulse generators.(1-6) The activities discussed in this review paper are in support of the needs in these areas and summarize much of the work currently under way in this country. The primary purposes of these programs are to

- determine qualitative component and system behavior in the microsecond and shorter multihertz repetition rate, high di/dt discharge environment,
- understand, model, and eliminate the failure mechanism that are observed in the above environment, and
- develop, in conjunction with industry, long-life, reliable components for use in the high di/dt , multihertz systems.

There is a pressing need for the development of very long life energy-transfer system components.(1,2,7) As additional applications of fast pulse power techniques are conceived, especially in laser technology, component specifications become more and more severe. High repetition rates, high peak and rms currents, and extremely high reliability are but a few of the difficult constraints. The basic components in pulsed power technology are capacitors, transformers, and switches. Recent progress in these areas will be discussed.

REPETITIVE COMPONENTS

Capacitors

The rationale in evaluating capacitor technology provided by industry is to determine and understand the failure mechanisms and then work with the manufacturers to develop advanced units.(2,3,5-7) This is in contrast to a basic research program to develop new dielectrics and impregnants. Rather, programs currently

under way generally seek to determine the capacitor system weak points, the characteristic failure mechanisms, and the required dielectric characteristics compatible with multihertz, high di/dt discharges.(3,5,7) The resultant data base should provide direction to future basic dielectric system research and development. A natural result of these activities is the determination of the operating limits of present capacitor technology in different capacitor structures.(7,8)

Programs have been under way in industry for some time, directed toward developing lightweight, high-energy density repetition-rate capacitors (≈ 100 Hz) for burst-mode operation.(7) In this situation the capacitor must operate for a few minutes at a time and recover during a several-hour quiescent period. Currently, ≈ 40 J/kg units are commercially available and in use in military systems.(7) Significantly higher energy density capacitors are in the developmental stage for continuous duty operation.(6) It remains to be seen just what is the limiting energy density for this application. The point must be made that ultimate achievable energy densities may be application dependent.(8,9) Thus, the user is cautioned.

The other class of applications is those wherein high-repetition rates (≈ 20 kHz) and multiyear lifetimes are demanded at submicrosecond discharge times.(2,3) These parameters for excimer laser isotope separation lasers are summarized in Table I.

TABLE I

CAPACITOR TEST PARAMETER RANGES

Parameter	Value
Capacitance	0.5-2 nF
Voltage	10-100 kV
Discharge time	60-100 ns
Reversal	10-15%
Pulse repetition frequency	0.1-5 kHz
Peak current	0.1-50 kA
Life (>99% confidence level)	10^4 - 10^{10} discharges

Because recent thyristor switch development has indicated that a higher level of performance can be achieved by pulse charging, capacitor development must be undertaken for both resonant charging (charging time, $\tau_c \approx 1/prf$) and pulse charging ($\tau_c \leq 5 \mu s$) conditions.(3) In addition, previous work showed a dramatic increase in lifetimes for such pulse-charged capacitors of the ceramic type(14), and it is reasonable to postulate that this may well be a property of capacitors in general, thus worthy of investigation in its own right. The general layout of such a dual mode test and evaluation facility is presented in Fig. 1.(2,3)

Perhaps the most important part of pulsed power technology is power conditioning. In the component development laboratory, both resonant and pulse transformer charging (command charging) are used to fully characterize the behavior of discharge components.

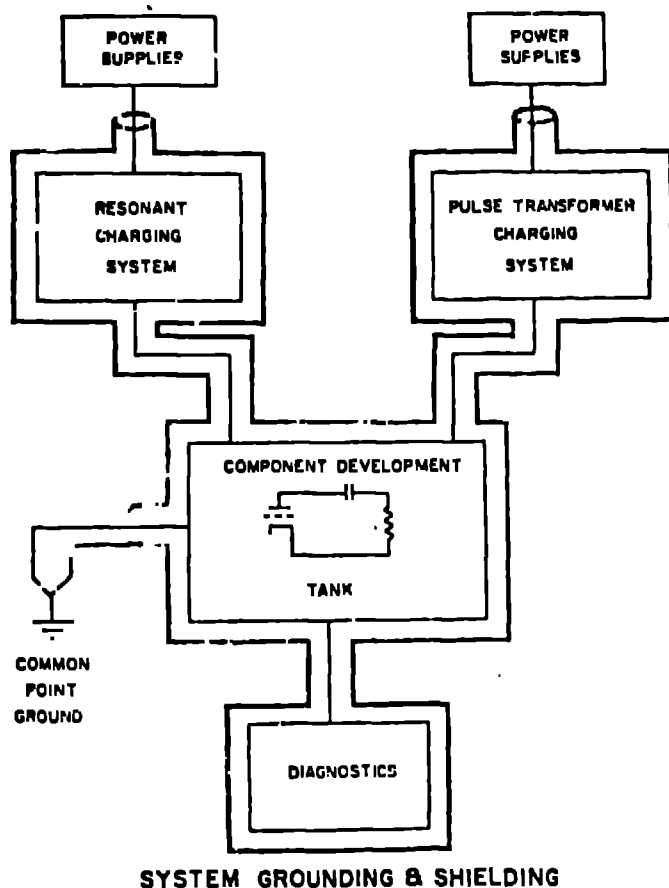


Fig. 1. High-repetition-rate component development laboratory operating system.

In the capacitor development program for laser isotope separation,⁽³⁾ linear resonant charge voltages of 5 to 60 kV at repetition rates to 3000 pps are available. With the use of saturating inductors, peak-charge voltages of 75 kV are achieved. Pulse-forming-network (PFN) capacitors up to 4 nF can be charged to 80 kV at 1000-pps repetition rates. At reduced operating parameters, capacitors of several microfarads can be operated in the discharge circuit.

Pulse transformer charging extends the operating range of the facility to a maximum charge voltage of 120 kV at repetition rates of 5000 pps. Capacitor values up to 15 nF can be charged in 2 to 10 μ s. Wall-plug efficiencies of 85% are achieved with present pulse transformer charging systems, and efficiencies of >90% are expected in systems under development.

Because the resonant and pulse transformer charging systems are completely separate, a discharge circuit under investigation can be rapidly changed from one to the other. The lumped equivalent circuit for one discharging capacitor is illustrated in Fig. 2. Circuit parameters are determined temporally during the discharge pulse duration by solving the time-dependent circuit equation iteratively, thus identifying pulse parameters having time variations. Except for the normally expected time varying resistance of the thyatron during the discharge time, only a modest dependence of C_c with time has been observed. At this time, it is not clear that the latter is of any significance. As high time and voltage resolution are demanded, the data are recorded on a multichannel transient digitizer. Thus each of five capacitor currents and voltages can

be measured and recorded sequentially by the data-acquisition system. A 100-kV voltage probe with a frequency response from 0-300 MHz has been developed for measuring the circuit voltages.⁽¹³⁾ Nanosecond response from the current viewing resistors (CVR) and voltage probes is required to monitor current fluctuations, and partial discharges (PD), in real time during the charge and discharge of the capacitor under test.

The data-handling capability of the data-acquisition system allows calculation of the following parameters during discharge:

- Circuit component impedance
- Component power flow
- Energy flow
- Equivalent series resistance of load resistor

The resolution of the diagnostic system is such that a change in circuit parameter values of 0.5% can be detected.

In the development of various high-voltage components, the area of prime interest is multihertz, long-life, low-inductance capacitors. A major program to fully characterize capacitors designed for pulse duty is in progress.⁽³⁾ The motivation for pulse-capacitor development is threefold:

- To obtain a data base to understand the physics and chemical processes affecting capacitor life.
- To develop low-loss, extremely long-life capacitors (>10¹² shots).
- To interact with industry in designing capacitors in the range of 1 to 20 nF, capable of 10-kA/nF peak current in 50- to 100-ns duration discharges.

There are at least two configurations that meet the low-loss requirements: silicon oil/polypropylene and reconstituted mica-paper capacitors.

The equivalent series resistance (ESR) is of prime importance in determining the loss of the capacitor during the discharge pulse. The ESR measurement was approached from several directions. The conventional

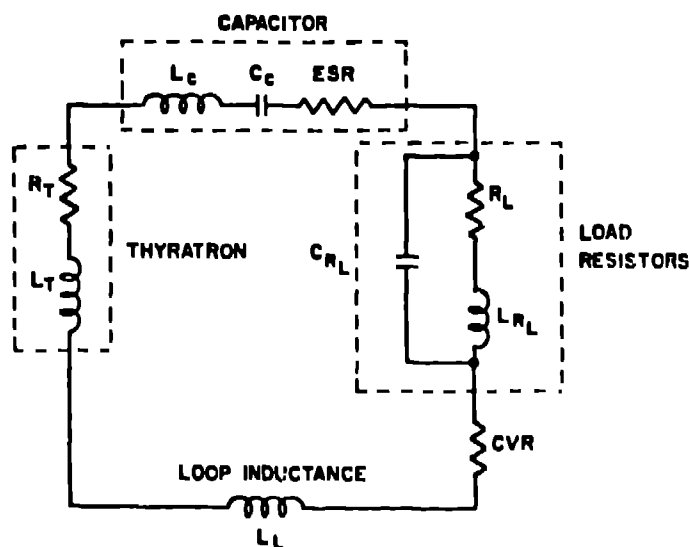


Fig. 2. Capacitor discharge circuit.

method of deriving ESR from a ringing discharge was used along with phase shift, Fourier analysis, and temperature variation measurements. A direct method using circuit theory applied to nonlinear, time-varying, second-order circuits was also used. Results from all methods indicated an ESR <100 mΩ. To make higher accuracy ESR measurements at 50-kV, 1-kA pulse levels at which the capacitors operate, a much higher measurement resolution (~0.02%) would be needed. In the polypropylene/silicone oil capacitors (PPSO), dependence of lifetime on repetition rate has been determined as seen in Fig. 3. The repetition-rate dependence is due to a time-voltage stress relation currently seen only in short-pulse high di/dt circuits. The two types of capacitors evaluated are illustrated in Fig. 4 for a 500-pF, 30-kV PPSO and 50-kV mica unit, both designed for kiloampere peak currents at kilohertz repetition rates, with discharge times 100 ns.

Capacitor Failure Observations and Data

Dielectric Degradation at Foil Edge

The failed PPSO capacitors, which were carefully disassembled, failed for the following reasons by approximate percentage:

- 5% defective fabrication
- 5% bulk dielectric failure
- 90% dielectric punch through at foil edge

The number of units that failed due to defective fabrication is somewhat above average. The bulk dielectric capacitor failures occurred around 10^6 discharges and were usually due to defects in the dielectric material. The remainder, and the majority, of the capacitors failed at the foil edge. The failure mechanism, illustrated in Fig. 5, consists of craters in the dielectric at many places along the foil edge that eventually eroded through the dielectric. Other observed damage, illustrated in Fig. 5, includes carbonization of voids in the dielectric between the foils and cratering at the foil edge.

Pressure-Dependent Foil-Edge Damage

Ninety per cent of the foil-edge damage occurred in the three outside wraps of the capacitor pack that were charged to the highest voltage with respect to

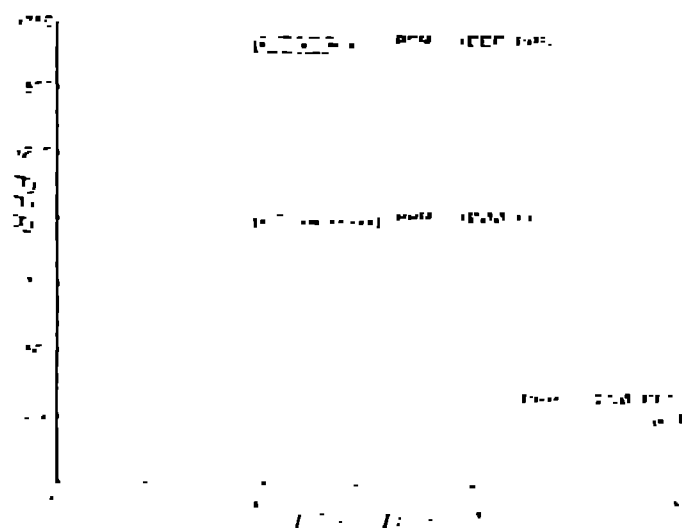


Fig. 3. Lifetime vs. pulse repetition rate for silicon oil/polypropylene capacitors for a 100 ns discharge time.

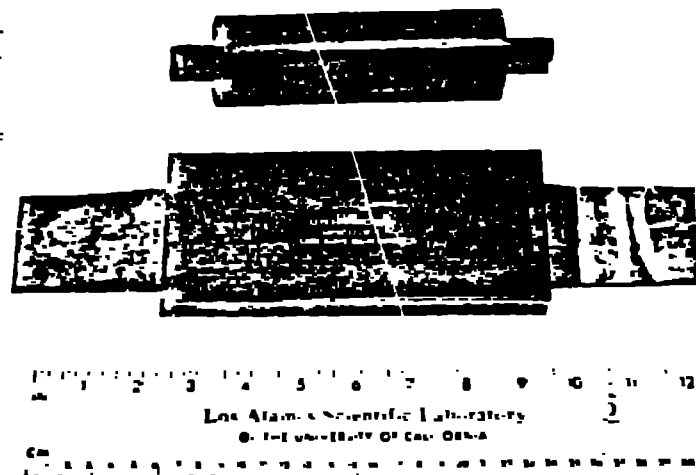


Fig. 4. Kilohertz, fast-discharge 500-pF capacitors: polypropylene/silicone oil is rated 30 kV, and reconstituted mica is rated 50 kV. The volumetric efficiency of the mica unit is superior.

ground or pack No. 1. The capacitor pack with the foil-edge failures was on the end of the capacitor connected to the thyatron anode. The foil voltage on this end of the capacitor changes from the charge voltage (~50 kV) to zero in approximately 40 ns and thus sees a large value of di/dt.

The damaged mechanism may have some relation to the transient current distribution during capacitor discharge. The capacitor pack can be used to illustrate the transient current flow. The discharge frequency is on the order of 10^4 Hz. The skin depth of the aluminum foil at 10 kHz is approximately equal to the foil thickness or 0.5 mil. Thus the charge stored in the interior of the capacitor cannot flow through the outer foils or the much thicker and higher resistivity solder connections on top of the foil to the edge of the capacitor. The charge therefore tends to flow in a spiral path to the pack edge in a strip transmission line formed by two capacitor foils.

Transmission-line effects may be responsible for dynamic voltage and thus electric field transients during discharge. (14) This suggests that during discharge, the peak electric field may be significantly

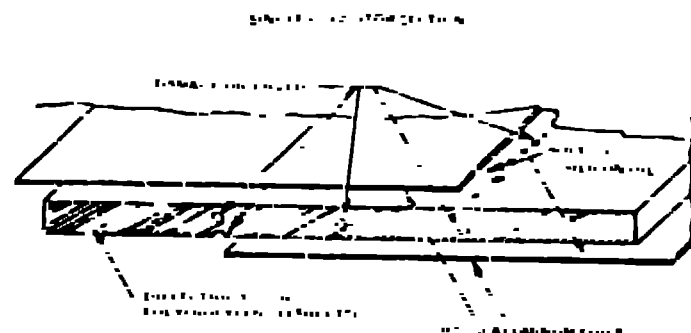


Fig. 5. Capacitor damage observed at kilohertz repetition rates.

higher than the average dc electric field. New capacitor pack connection designs that minimize current flow problems are being manufactured for test.

A second mechanism, which may produce the location-dependent PD damage, is the time rate of change of voltage (dV/dt) on the capacitor foil or pack with respect to ground. The capacitors tested were fabricated with an insulating phenolic case. Thus the outside foil is electrically in a low-inductance circuit, are capacitively coupled to ground through stray capacitance. The stray capacitance is charged during the relatively slow resonant (1 ms) charging time of the test capacitor. Simultaneously, the high field at the edge of the foil can inject free charge into the margin region of the capacitor. When the capacitor is discharged, (≤ 100 ns) the free charge in the margin coupled to ground through stray capacitance is at the original capacitor potential while the foil is now grounded. This situation can conceivably produce extremely high local electrical fields between the free charge in the margin and the foil edge. These high electric fields can also produce corona and dielectric degradation.(3,14)

Scanning Electron Microscope/Ion Microprobe Observations

Sections of the damaged dielectric were analyzed with a scanning electron microscope/ion microprobe system. This device allowed identification of the materials in the sample at atomic levels. The microprobe results indicated that the foil edge damage shown in Fig. 5 as cratering is an organic compound similar to the polypropylene dielectric. The black material is surrounded by a large amount of elementary hydrogen gas and a small amount of atomic oxygen, carbon, and silicon. The oxygen and silicon are probably the result of dissociation of the silicone oil impregnant. Analysis of the visible inclusions revealed they were small hydrogen gas bubbles surrounding black organic compounds similar to polypropylene, all of which are inside the section of 1-mil polypropylene film. This damage also occurred at the foil edge. The ion microprobe analysis found no aluminum in areas of dielectric degradation.

When the test capacitors were discharged at a peak current of 1 kA in an 80-ns-wide near critically damped pulse, and a 1-kHz repetition rate, the PD inception stress level was observed to be only 875 V/mil. The onset of these PDs during discharge was monitored by the facility diagnostic system as high-frequency information on the current trace (that is, oscillations) as shown in Fig. 6. In the test facility, the presence of PD is also detectable as very high frequency electromagnetic noise on the voltage pulse.

PD inception is observed as an integrated effect. When operating the capacitor above the inception level, PD is not observed for some time, T_i . If capacitor operation is halted after time, T_i , and resumed in a few minutes, PDs are immediately observed. If, however, capacitor operation is halted after PD observation for longer periods of time, say 24 h, and then resumed, there is a delay until PDs are again observed, but the delay is less than the initial delay. This reduction in delay time apparently continues over many start-stop-wait test cycles until the PD inception delay time, T_i , approaches zero. The appearance of PD is assumed to be the result of dynamic surface charge effects and is currently under investigation. The damage observed occurs at the edge of the foil, and the electric fields apparently also generate gas by dissociation of the impregnant and modification of the dielectric in regions of poor impregnation, bulk dielectric flaws, and high field. The renewable delay time or PD hysteresis effect with inactivity may presumably be related to the

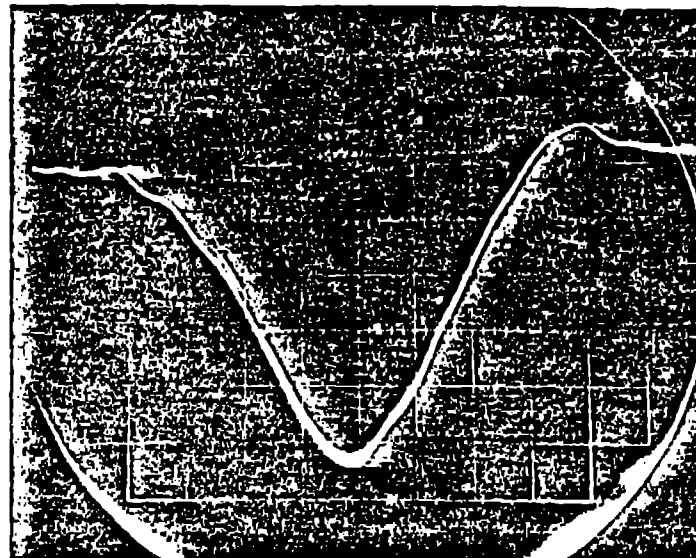


Fig. 6. High-frequency, partial-discharge oscillations evident on the leading edge of a 80-ns-wide current discharge pulse from a 500-pF polypropylene capacitor at a 1-kHz repetition rate.

solubility of the gas in the impregnant. The event of zero PD onset delay after a quiescent period occurs when the local impregnant is saturated with gas. After zero PD onset time delay, the internal gas pressure increases until the case explodes.

Repetition-Rate Frequency Effects on Internal Partial Discharges

The presence of PD was also found to be a function of and exhibited a hysteresis effect dependence on the discharge pulse repetition frequency (PRF). After the PD inception time delay, T_i , the PRF was increased from 100 Hz, where no PDs were observed, to 500-600 Hz where broadening was observed on the current trace. In order to extinguish the PD, the PRF had to be reduced below 250-350 Hz. This can be tentatively explained again as an enhanced electric field at the foil edge that dissociates gas from the impregnant (silicone oil). If the e-folding ($1/e$) deionization time of the gas generated by the field at the foil edge is on the order of 1 ms, the residual ionization level due to one discharge pulse would be less than that required to affect the subsequent pulse ionization level if the subsequent pulse is spaced 3-ms (330 Hz) or $3(1/e)$ times later. If this hypothesis is valid, discharge pulses spaced < 3 ms apart would generate more ionization and gas than the previous pulse due to the initial ionization present. This hypothesis could also explain the observed hysteresis effect if the total amplitude of the ionization process increases in time for pulse spacings less than the e-folding ($1/e$) deionization time. In this case, the time required for the residual ionization level to decay below that required to influence the next pulse ionization process is longer, even though the e-folding time is the same.(8,14)

Life vs Discharge Pulse Repetition Frequency

The life of PPSO capacitors is quite dependent on the discharge PRF and is probably related to the PD dependence on PRF. A plot of capacitor life vs PRF (Fig. 3) indicates that the life of a capacitor increases drastically below ~500 Hz, the repetition frequency at which PD is observed.

Once these PPSO capacitors were operated in the PD regime, the life was limited to approximately 2.8×10^6 discharges regardless of PRF. This indicated that PD damage is accumulative. On the other hand, PPSO capacitors, when operated at lower dV/dt and lower di/dt , have functioned for greater than 10^{10} shots in other parts of the test facility.

The Weibull distribution analysis of the failures indicated a single failure mechanism was responsible for failure, and the failure distribution was very narrow ($<1\%$).

Capacitor Energy Dissipation

Initially, the dielectric loss and the ESR of the capacitor was of major concern. However, the energy dissipated in the capacitors tested was so minimal that thermal effects were negligible. For comparison, the temperature rise of a conventional Mylar paper capacitor is compared with that of a Teflon unit (Fig. 7). Both units were operated at a discharge PRF of 1 kHz, a peak current of approximately 1 kA in a 100-ns-wide pulse. The test was halted after 42 min when the Mylar paper capacitor exploded due to the 65°C temperature rise compared to the 4.1°C temperature rise for the Teflon unit. The mica, Teflon, and PPSO capacitor units have a dissipative component so small that at present rms current levels up to 15 A, a maximum of only 10°C temperature rise above ambient were observed.

Data for the mica capacitor were not obtainable, as no units failed under the test conditions available in the facility. They also passed a 150-kV hi-pot test.

Present Repetitive Capacitor Technology Base

The performance evaluation of low-inductance types of capacitors in the 100-ns, 1-kA, 1-kHz regime has led to the following observations:

- A high-quality, high-frequency diagnostic system is essential to observe transients within capacitors during discharge. The high-frequency CTRs and voltage probes developed for the system are required diagnostic tools.

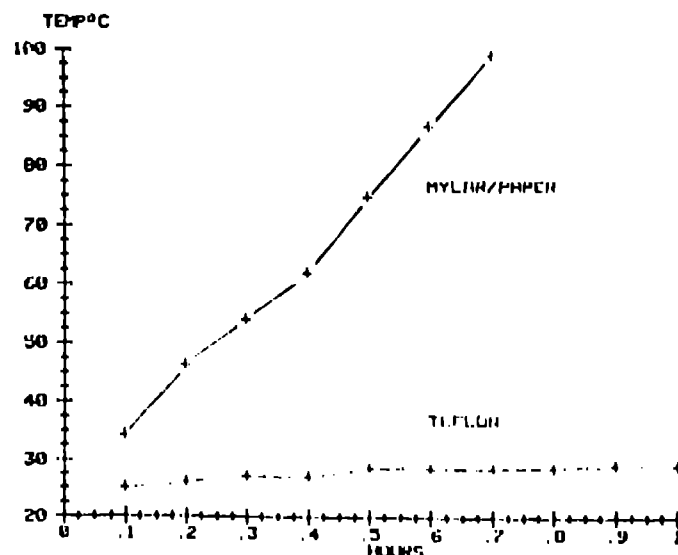


Fig. 7. Temperature rise of Teflon and Mylar paper capacitors operating at 1-kHz PRF and 100-ns discharge time.

- PDs are the main cause of failure in PPSO capacitors and are detectable during discharge. (15)

- The PD inception stress level during discharge is about 25% of the dc level and is dependent on time duration of discharge and the pulse repetition rate.

- Preliminary tests indicated that Teflon-silicone oil and mica-paper capacitors had a longer life in the regime tested than the polypropylene-silicone oil units, but with lower energy density. This is attributed to the impregnation characteristics of Teflon units and fabrication methods of the mica units and may not represent intrinsic limitations.

- Capacitor power losses are negligible for units designed for this regime.

- Present fabrication techniques must be modified to accommodate the transient currents and voltages within the capacitor.

The PPSO capacitors were initially evaluated in detail because of the energy density potential, their availability and low cost, and the assumption that similar failure mechanisms would occur in the Teflon and mica-paper units, but at longer accumulated life.

In the future the Teflon and mica-paper units will need to be stressed at higher levels to assess their lifetimes and thus determine their characteristic failure mechanisms.

Pulse Transformers

One of the major advances in transformer technology has been the recent development in air-core pulse transformers. Air core pulse transformers are typically found in applications involving very high peak power levels (up to 10^{11} W) or ultrahigh rf. They differ from the more common iron or ferrite types in that no ferromagnetic materials are used to channel the magnetic flux through the winding to assure flux linkage. With air-core transformers, flux linkage is strongly dependent upon the physical proximity of all turns of one winding with respect to all turns of the other winding. Consequently, the coupling coefficients of air-core transformers tend to be lower than magnetic core transformers, particularly with high-gain transformers that have thick, multilayer windings, however, because air-core transformers do not have magnetic cores they are not limited in current-handling capacity by saturation of the magnetic materials or frequency limited by the composition of the core. Not having core saturation and frequency limits are the two most significant advantages of air-core pulse transformers. They are, therefore, well suited for use with large, high-current primary pulsed power sources such as parallel capacitor banks, which often operate at peak current levels of over a megampere and also in such applications as high-voltage triggering where the discharge frequency may be several megahertz. This discussion will cover only the general types designed for high-voltage pulse generation and energy transfer applications. Special emphasis has been given to pulse-charging systems that operate up to the multimegavolt range.

Types of Air-Core Transformers

There are two basic types of high-voltage air-core pulse transformers that can be operated in the megavolt range. The first and most common is the single-layer helical-wound transformer (Fig. 8). The second is the spiral-strip type (Fig. 9). These transformers differ

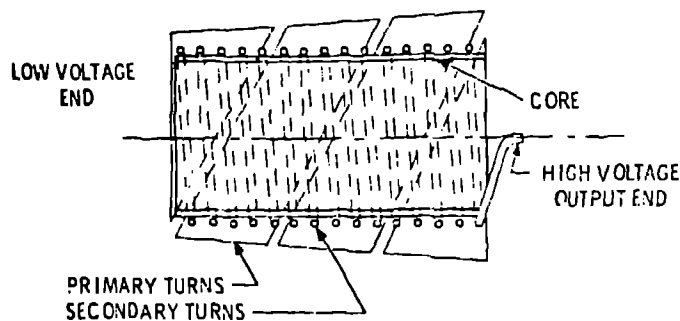


Fig. 8. Basic helical wire transformer.

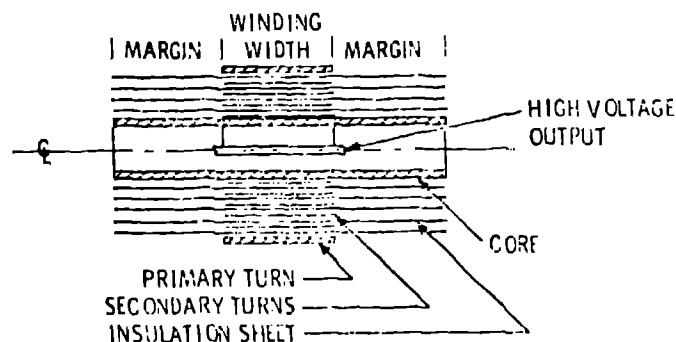


Fig. 9. Basic spiral-strip transformer.

from each other primarily in the configuration of the secondary windings; that, as will later be shown, accounts for a significant difference in their resistance to insulation failure from fast pulses. The primary windings for either type, however, whether single or multiple turn, may be designed in a variety of ways without affecting electrical breakdown characteristics of the transformers. For reasons of high-voltage isolation, the low-voltage primary winding is typically placed outside the secondary in either type transformer so that the high-voltage output of the secondary may be led out through the center of the assembly.

With helical transformers, high-voltage standoff between the primary and secondary windings is provided by an insulated space between the windings. This separation may be uniform or tapered in the longitudinal direction. When tapered, the insulation thickness (usually oil) increases with the voltage along the length of the coils so that the electric stress remains constant along the length of the windings. With spiral-strip transformers, voltage standoff is largely a function of the radial thickness of the secondary winding because the primary and secondary turns directly overlay each other. The winding stack therefore has a pure radial voltage gradient between the high voltage inner turns and low-voltage outer turns. Like helical type transformers, the open volume in spiral-strip transformers is usually insulated with oil. However, because of the high winding density, spiral-strip windings must ordinarily be vacuum impregnated to displace air from the secondary winding.

Two problems are common to both types of transformers:

- Electrical breakdown turn-to-turn or between windings

- Energy losses from eddy currents induced in voltage grading devices and structural components that are present in high-voltage transformers.

Turn-to-turn breakdown is common to helical transformers when used in charging systems for pulse-forming lines (PFL). This problem arises from fast-rising (usually ≈ 10 ns or less) voltage transients generated by the discharge of the PFLs, which are fed into the output of a direct coupled transformer. The turns of a helical winding are inductively and transit time isolated from each other and so the capacitive components between turns and from each turn to ground (Fig. 10) are not sufficient to grade fast-rising transients. Consequently, a voltage pulse approaching the full amplitude of the transient can momentarily appear across the final turns of the secondary and cause breakdown. This problem was corrected in the FRIZZ transformer design(17) by adding a capacitive voltage grading dish across the output turns of the transformer as shown in Fig. 11.

By contrast, spiral-strip transformers are inherently less prone to breakdown from fast-voltage transients because the interturn capacitance components are all directly in series to ground as shown in Fig. 12.

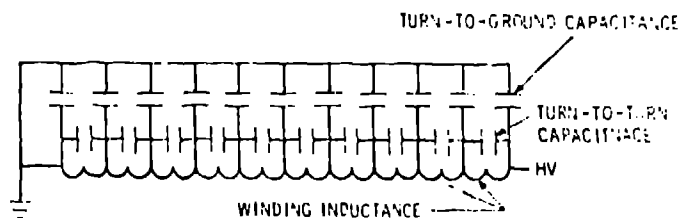


Fig. 10. Equivalent circuit along the length of a helical-wound transformer.

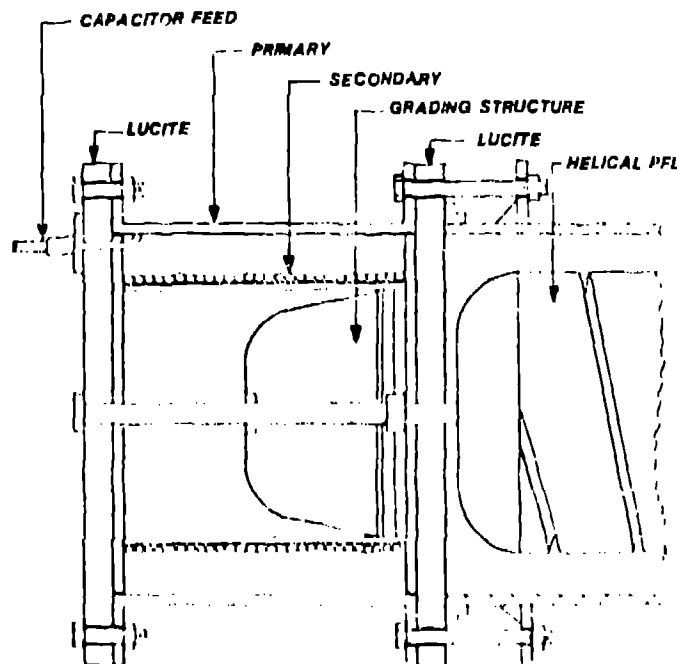


Fig. 11. FRIZZ helical transformer.

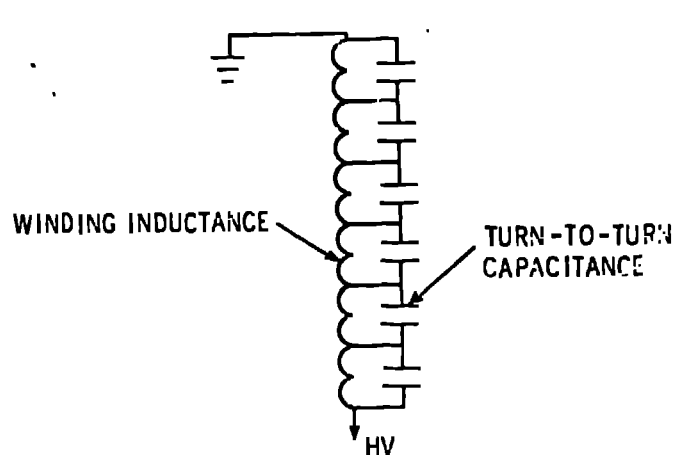


Fig. 12. Equivalent circuit through the thickness of a spiral-strip winding.

They are comparatively large because of the large surface area and close spacing between turns of the spiral strip. Consequently, a fast-voltage pulse is capacitively graded through the thickness of the winding. The principal weakness of simple spiral-strip windings, however, is their tendency to break down at the thin edges of the strip. An arc breakdown typically originates from the edge of one of the final high-voltage turns, flashes across the insulation margin, and closes the discharge path to the low-voltage primary. Such breakdowns practically always damage the insulating film in the margin and leave a heavy carbon path through the oil.

These edge breakdowns result from highly enhanced electric fields associated with equipotentials that emerge from between the high-voltage turns and bend sharply around the edges toward the low-voltage turns (Fig. 13). The high fields can be significantly reduced and edge breakdown eliminated by placing a coaxial shield across the margins to shape the equipotentials into a coaxial distribution that is nearly parallel to the uniform field through the thickness of the winding, Fig. 14.

Adding the voltage grading structures to either type of transformer can lead to the second major difficulty with air-core transformers, which is increased

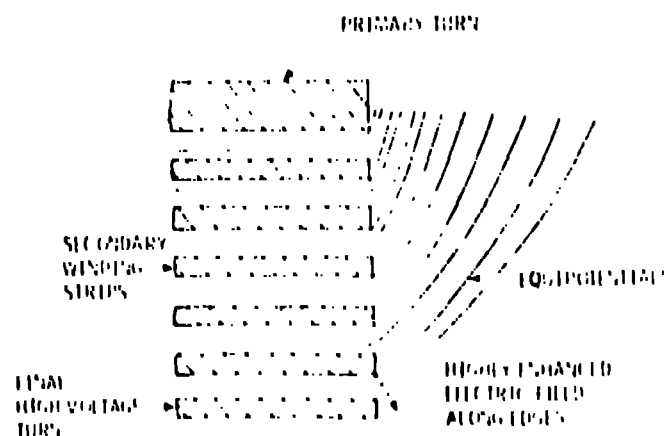


Fig. 13. Equipotential profile at the edge of an unshielded and ungraded spiral winding.

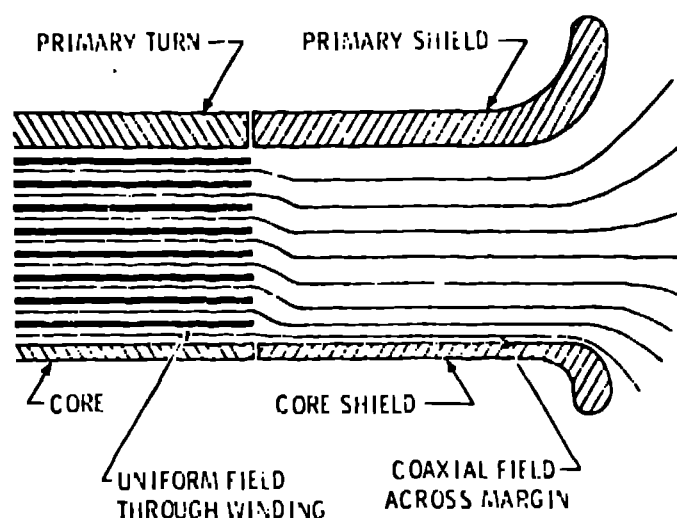


Fig. 14. Coaxial shield across spiral strip transformer margin.

eddy current losses in the transformer grading structures. Although these structures may be slotted, eddy currents can be induced as illustrated in Fig. 15, a diagram of eddy currents in cylindrical shields around the margins of a spiral-strip transformer. The effect of eddy current shorting is to decrease the voltage gain and energy transfer efficiency of the transformer by an amount roughly proportional to the magnitude of the eddy currents. In one instance, cylindrical shielding reduced the gain of a spiral-strip transformer by 58% compared to an equivalent unshielded transformer.(18)

Electrostatic shielding and grading structure designs must therefore be concerned with making them transparent to magnetic fields. One grading technique that has been employed successfully with transformers used in single-shot service is to fill the open volume of the transformer with a resistive liquid such as water or a solution of water and copper sulfate.(19,20) In these cases, voltages are resistively graded but the resistivity of the solution is sufficiently high so that no current of any magnitude can be induced in the solution during the time of energy discharge. Resistive solution grading is adequate for single-shot transformers but less satisfactory for repetitive pulse applications because of resistive power losses in the grading solution.

The most successful method(21) developed for grading spiral-strip transformers is the use of concentric

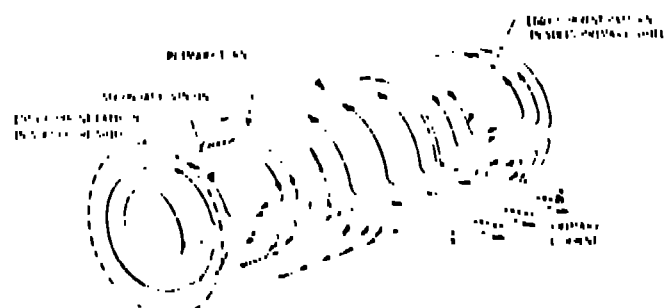


Fig. 15. Eddy-current pattern in solid concentric shields.

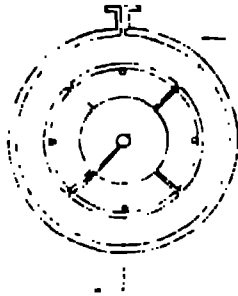


Fig. 16. Ring cage shield for spiral-strip transformer.

ring cage shielding across the margins as shown in Fig. 16. Magnetic fields diffuse freely through the ring cage without inducing eddy currents in the elements and yet maintain the proper electric field distribution in the margins. Each ring, of course, must have at least one circumferential gap to prevent current from flowing in the hoop direction of the rings. Spiral-strip transformers shielded in this manner have been operated successfully in PFL charging applications to 3 MV with over 90% energy transfer efficiency from the primary to secondary capacitors. (21,22) Figure 17 is a diagram of a ring shielded transformer that operates with high efficiency (>90%) at the multimegavolt level.

Transformer Circuit Analysis

Pulse transformer circuits often utilize capacitor banks as the primary energy store. One of the principal reasons is that capacitors are capable of develop-

ing higher peak power levels than any other electrical device. The transformers in these circuits must therefore be capable of delivering the intense primary power pulse to a load on the secondary at a higher voltage or higher current with a predetermined transformation ratio. For transformers with perfect coupling, no winding resistance, and negligible interturn capacitance (Fig. 18), a simple set of relations may be derived that relate the primary and secondary current (I_P , I_S) and voltage (V_P , V_S) to the primary and secondary turns (N_P , N_S) of the transformer:

$$I_P N_P = I_S N_S \quad (1)$$

$$\frac{V_P}{V_S} = \frac{N_P}{N_S} \quad (2)$$

The primary and secondary impedances (Z_P , Z_S) are:

$$Z_P = \frac{V_P}{I_P} \quad (3)$$

$$Z_S = \frac{V_S}{I_S} \quad (4)$$

from which

$$\frac{Z_P}{Z_S} = \left(\frac{N_P}{N_S} \right)^2 \quad (5)$$

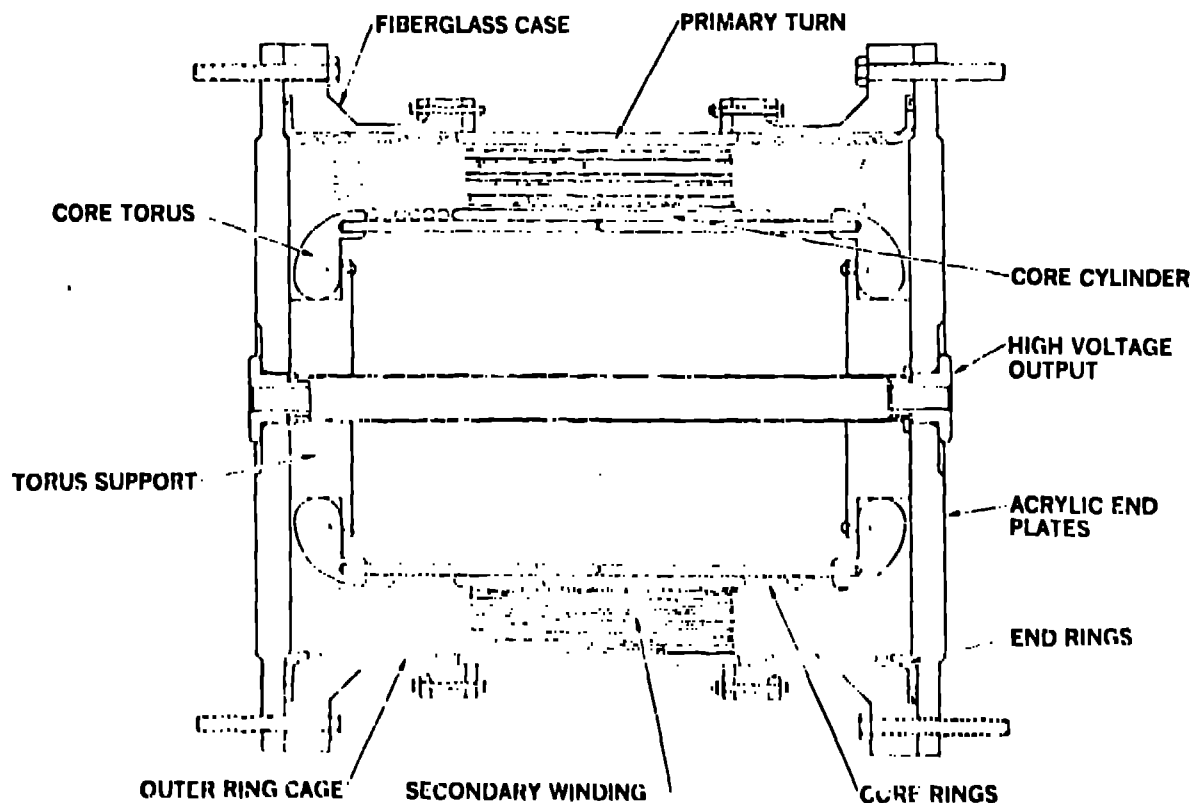


Fig. 17. A complete 3-MV oil immersed spiral-strip pulse transformer.

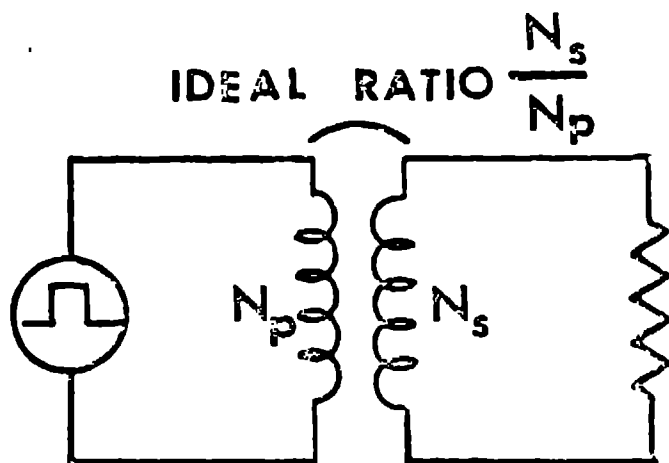


Fig. 18. Basic transformer circuit.

From these ideal relations, it can be seen that a transformer can be used to change current, voltage, or impedance. However, because no transformer is perfect and often both the primary and secondary sections of the circuit have resonant characteristics, the detailed analysis of such circuits is somewhat more complex.

Of present interest are transformer circuits where low-voltage capacitor banks are used for charging high-voltage pulse forming transmission lines by means of a voltage step-up transformer (Fig. 19). Such charging circuits may be operated in matched- or off-resonance modes,(18) but are generally matched as nearly as possible to maximize energy transfer efficiency. In the matched frequency mode, that is, with the open circuit frequencies of primary and secondary sections of the circuit equal ($L_p C_1 = L_s C_2$), two cases shown in Fig. 20 are of practical interest:

- swing charging where maximum secondary voltage is reached on the first excursion
- dual resonance charging where maximum voltage occurs on the second or reverse voltage excursion of the secondary.

Analysis shows that any transformer with a coupling coefficient >0.6 can be adapted to a dual resonance circuit. Unless the circuit coupling is close to 1.0, it is more advantageous from the standpoint of transfer efficiency to operate in the dual resonance mode(21) with $K = 0.6$. With repetitive pulse systems, high-transfer efficiency is essential to preventing excessive energy dissipation in the system components from residual energy ringing through the system after

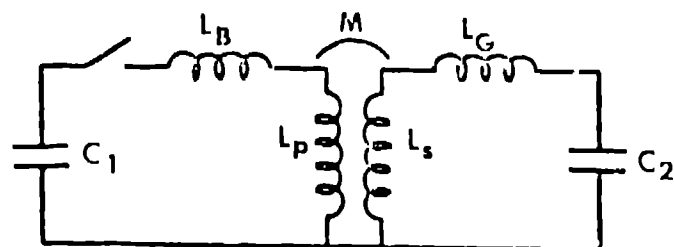


Fig. 19. Basic pulse transformer charging circuit.

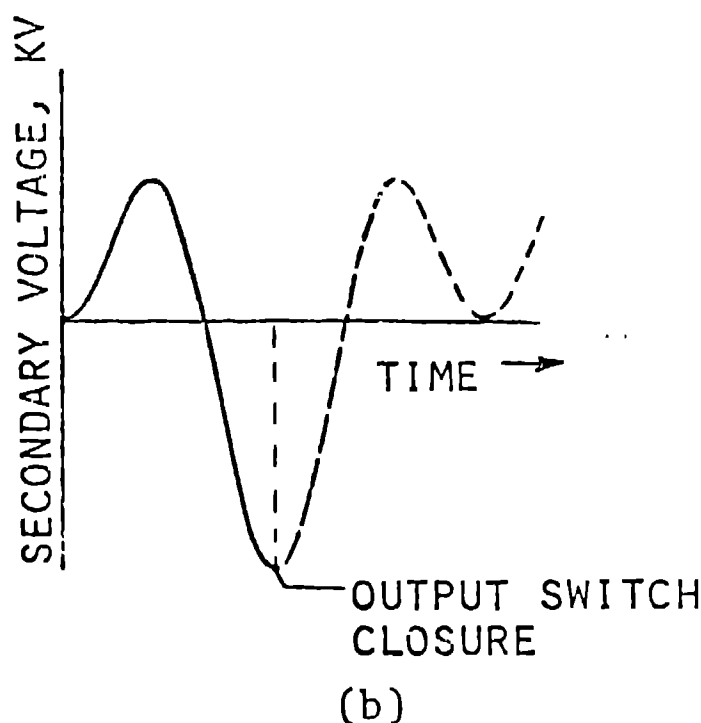
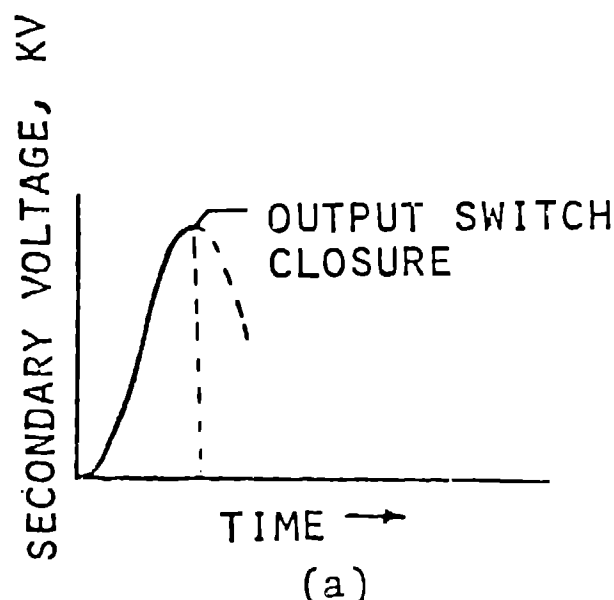


Fig. 20. (a) First-swing charge cycle
(b) Dual resonance charge cycle.

discharge of the secondary capacitor. When properly tuned, dual resonance charging systems will operate with an overall efficiency between 90 and 95%.(21,22)

Switches

The proper choice of switches for a given application depends upon both the system requirements and the specific capabilities and limitations of the switches under consideration. Gas-insulated spark gaps and hydrogen thyristors are two types of switches commonly used in single-shot and repetitive pulsed power systems. These switches have overlapping capabilities but differ in their optimum ranges of voltage, current, peak power, repetition rate, turn-on speed (di/dt), recovery rate, and operating efficiency.

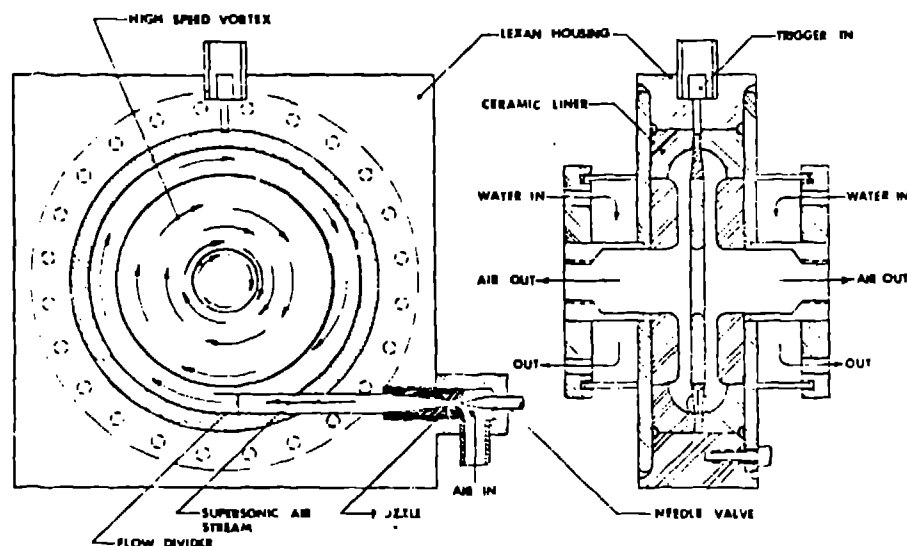


Fig. 21. A 60-kV vortex-flow gas dynamic spark gap designed to switch 2 kJ at 100-Hz PRF.

In general, spark gaps have higher current, voltage, peak power, and di/dt capabilities than thyratrons, but thyratrons are presently capable of higher average powers, repetition rates, faster recovery, and higher operating efficiency in repetitive systems. These are a few of the factors that must be considered in the selection of switches for various applications. Development is proceeding in all areas of switching, which will eventually extend the capabilities of familiar switches such as spark gaps and thyratrons but quite possibly result in the introduction of new switching devices and techniques such as ultrafast magnetic switches.

Spark Gaps

Gas-insulated spark gaps of various designs are used in a wide variety of pulsed power systems that range in size from a few joules to multimegajoules. Operating voltages range from as low as 1 kV to several megavolts and peak currents from a few tens of amperes to several megamperes. Thus, spark gaps are perhaps the most versatile type of currently available high-voltage switches insofar as their spectrum of applications. Spark gaps are most often used in single-shot systems but can readily be adapted to repetitive pulse service by flowing insulating gas through the switch volume to carry away shot-to-shot ionization debris. Figure 21 is an example of a 60-kV gas dynamic spark gap designed by Rohwein to switch 2 kJ at a repetition rate of 100 Hz.

In addition to their simplicity and comparatively low initial cost, the principal advantages of spark gap switches are:

- Fast turn-on time to approximately 10^{11} A/s.
- High-current capacity of 100 to 100 kA per current channel
- Ability to conduct ringing discharges
- Wide operating range with internal pressure control
- Losses limited to approximately 5% with microsecond or longer pulses

Disadvantages include:

- Life limited by electrode erosion to 10^7 to 10^8 shots
- High-volume gas flow required for repetitive pulse operation
- Repetition rate limited to approximately 1 kHz
- High resistive losses (10 to 30%) for nanosecond pulse durations

Little progress has been made to date in developing high-repetition-rate spark gaps having low commutation losses. The most recent data show losses from 10 to 30% per pulse and erosion-limited lifetimes $\sim 10^7$ shots. Erosion in itself as a lifetime factor is amenable to geometrical remedies, such as using consumable electrodes. Resolving triggering degradation, jitter, and commutation loss increasing with accumulated shots are only some of the factors being very actively investigated in gas switch research and development programs around the country.

Thyratrons

High-average power switching is emerging as a major area in the field of pulsed power. To meet the requirements of long life, high-repetition rate, and low loss, the thyatron at present is the only viable choice. In addition to the above qualities, thyratrons require less support equipment than high-repetition-rate spark gaps and are far more economical to use. Areas of present thyatron investigations include efficiency, power and energy flow, and switching characteristics.

One of the major problems to date in fast-discharge, kilohertz repetition-rate spark gap switching is the large losses experienced in the switch. In long-life, high-reliability circuitry such losses are totally unacceptable. The thyatron losses during commutation in a low-energy, fast-discharge circuit have been measured.⁽²⁾ For stored energies of 0.5 to 1.2 J, this loss is 2% at an 80-ns pulse width and a peak current of 700 A, as shown in Fig. 22. The losses were observed to decrease rapidly with increasing energy, as

ENERGY DISSIPATION IN THYRATRON (HY5322)

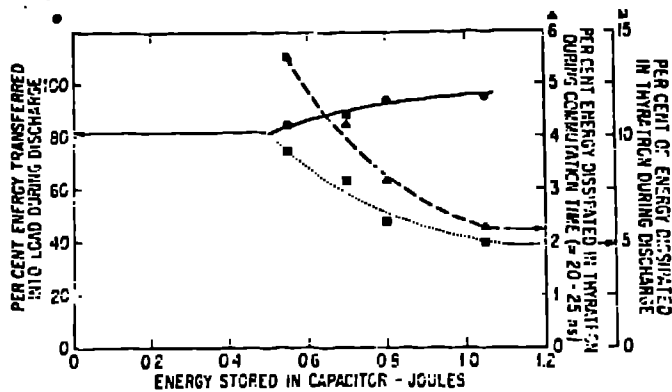


Fig. 22. Commutation and total discharge time energy loss for an EG&G low-inductance hydrogen thyatron as a function of energy stored in the capacitor. The peak current was ≈ 700 A and the pulse width 80 ns.

expected, so that low-loss switching is feasible with thyratrons, giving long economical life at high switching efficiencies. Retention of these low energy losses remains to be confirmed at higher energy levels (~ 1 kJ).

New, compact, short-pulse thyratrons are currently under development for 50 to 100-kV multikilohertz operation at current rates of rise in excess of 10^{12} A/s at 10- to 100-kA peak-current levels. The newest 3-in. low-inductance thyatron currently under detailed study(3) is shown in Fig. 23, along with the recently developed T&M, Inc., integral current-viewing resistor and di/dt monitor.

Table II tabulates salient features of present thyatron applications.(23)

The peak stand-off voltage vs pulse current for large commercial thyratrons shown in Fig. 24 is taken from T. R. Burkes' extensive switching report.(24)

Characteristics of developmental tetrode thyratrons are presented in Table III, clearly showing the major advances recently made in the field.

Switch Summary

Hydrogen thyratrons have many advantages when all things are considered. No other switch is yet capable of switching the same average power (1 MW) at the same efficiency ($>90\%$) on a continuous basis.(25) High di/dt and pulse repetition-rate capabilities along with reasonably long life (2,000 to 10,000 h) make the thyatron invaluable in many applications wherein no other switch has all these demonstrated capabilities.(26) Even so, improvements in hydrogen thyratrons are continually being made.(27)

A further significant improvement could be made if a scheme can be found to better utilize the capabilities of the cathode. Such an improvement could lead to higher di/dt as well as peak current capabilities. An improvement in the emissivity of the cathode material would allow higher peak currents to be drawn. It has been many years since significant advances have been made in cathode capabilities.(28)

The capabilities of some switches have been greatly increased by the use of optical triggering tech-

niques, for example, laser-triggered spark gaps and silicon-controlled rectifiers. A similar technique may be applied to the thyatron. This technique might eliminate the effects (delay and jitter) incurred by the necessity of propagating a plasma and greatly increase the di/dt capability and cathode utilization of thyratrons.

Higher voltages in single-gap tubes have been achieved.(29) Current packaging techniques do not make use of this technology. Needs to date have emphasized low inductance and high-average power more than voltage capability. The latter is now becoming an active research and development area.(27)

Numerous applications requiring very low jitters are arising. Recently, high pressure, low-inductance thyratrons have been developed(30) to meet multikilovolt level nuclear particle diagnostic requirements for

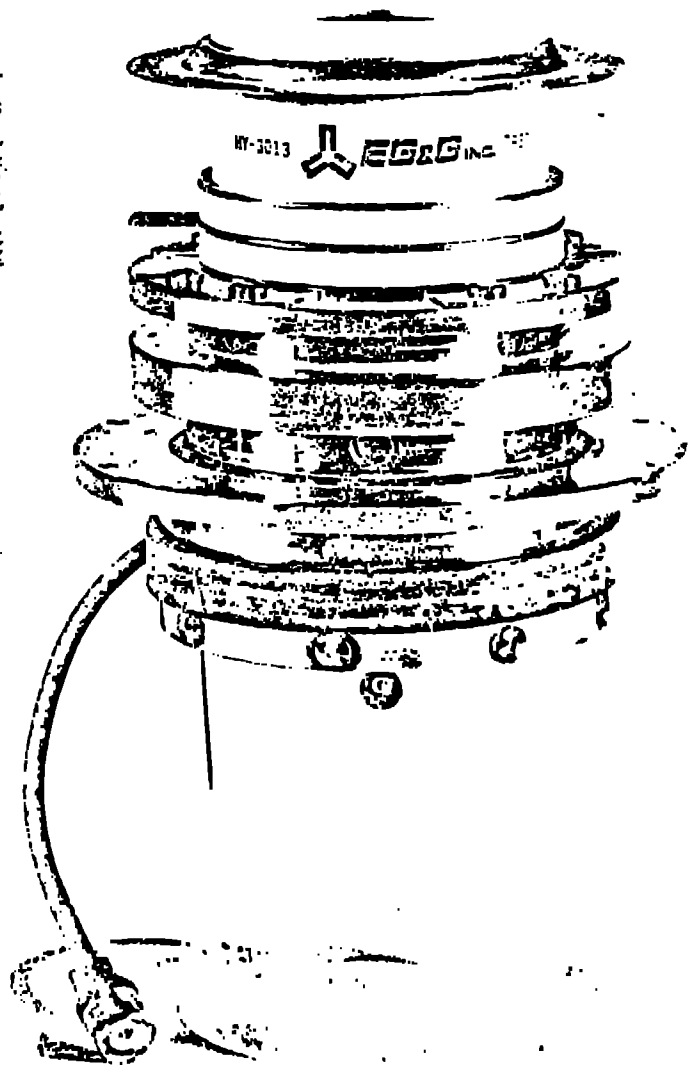


Fig. 23. Low-inductance thyatron with integral commercial current-viewing resistor and di/dt monitor.

TABLE II
TYPICAL APPLICATIONS SHOWING WIDE RANGE OF REQUIREMENTS

	Small Lasers		Pulsed Gas Ultraviolet Lasers	Isotope Separation (Proposed)		Adiabatic Mode	
	Target Deuterium Laser	Neodymium Laser		LiF	Los Alamos	Maps 250	Maps 250
Anode voltage, v_{py} (kV)	20-30	4	15-35	15-30	20-30	250	250
Peak anode current, I_p (kA)	0.4-2	0.015	20-30	0.1-4	10-20	20	40
Average anode current, I_a (Ade)	0.065	0.015	0.001-0.1	1-10	5-10	2	50
RMS anode current, I_p (Ade)	3	0.5	5-100	10-100	20-300	200	1400
Pulse width, t_p (ns)	0.2-0.5	0.1	<0.1	~1	~1	2	10-20
Repetition rate, prf (kHz)	0.015	10	0-10	10-50	~1	0.05	~0.5
di/dt (kA/ns)	2	1.5	≤1000	~100	60-100	30-50	20
Average power (kw)	0.02-0.1		0.05-1	20-100	50-100	500	1000
Major limits or problems	● No heater power is a requirement		● Switch inductance	● High prf	● High peak current	● High voltage	● No kickouts allowed
			● Switch resistance	● Recovery requirement	● High peak current	● High peak current	● High peak current
				● Unknown dissipation	● Life		● High peak current
				● Life			● Heater power

TABLE III
CHARACTERISTICS OF DEVELOPMENTAL TITANIUM THYRATRONS

	Standard Devices	Developmental Devices						
	Standard Triodes	New Low-Inductance Design Resonantly Staggered	Pulse- Charged	New Very Low Inductance Concept Pulse-Charged	Multiple Gradient Grid Tube	Large Cathode Type	New Large Cathode Gradient Grid Tube	Long Pulse Tube
Representative Grid tubes, resistive falltime to 1/e, ns	HY5 4	HY53 3	HY513 2	— 1	HY554 4	HY7 4	— 4	HY413 4
Inductance, nH	50	15	10	2	60	50	<100	100
Voltage, v_{py} , kV	1-70	1-35	1-40	1-100	1-250	1-40	>250	1-250
Peak current, I_p , kA, for pulse widths								
(a) ≤100 ns	20	20	20	200	100	200	300	—
(b) 1-20 ns	5	6	6	80	20	80	100	—
(c) ≤20 ns	8	8	8	20	15	20	100	20 A
Average power, kW	50	50	50	2000	250 500 (burst)	500 1000 (burst)	2000	2000 (one every 3 min)
RMS current	120	120	120	1000	1000	1600	1000	80
Average current	5	5	5	20	15	20 50 (burst)	100	80
di/dt, kA/ns	5	10	400	>2000	10	150	500	NA
Note: Rated peak inverse voltage, kV, for pulse widths				<100 ns 25 kV 1-20 ns 15 kV 20 ns 20 ns 1 kV				

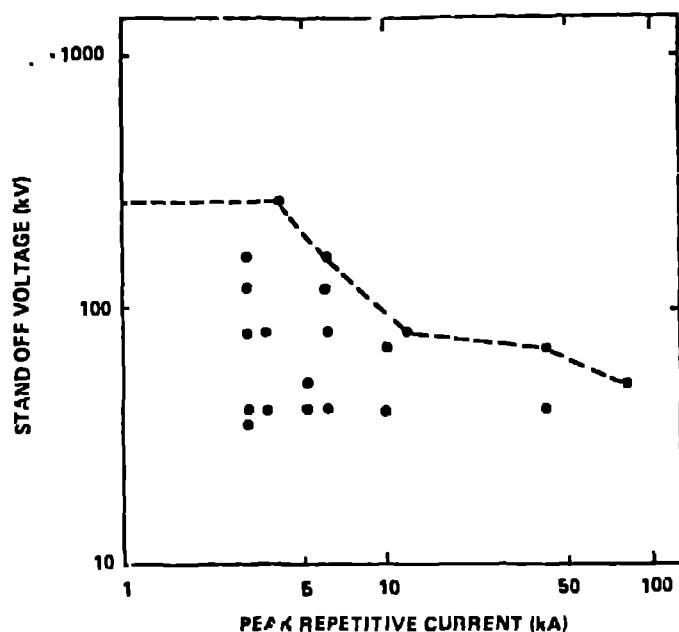


Fig. 24. Peak stand-off voltage vs pulse current for large commercial thyratrons.

stable delay time, fast switches. In Fig. 25 the system jitter from input to 5-kV high-voltage output is presented as a function of thyatron peak trigger voltage. Recent measurements have demonstrated system peak-to-peak jitters of significantly less than ± 30 ps. This opens previous single-shot areas to repetitive operation in many accelerator and laser applications.

INSULATION

The environment in which high-voltage components are placed does have thermal as well as electrical breakdown implications. Generally, most developmental high-repetition-rate systems employ oil rather than gas for insulation in order to achieve adequate component cooling. For high-voltage transformer oil, such as Shell DialaX, the dielectric strength as a function of water contamination is illustrated(31) in Fig. 26.

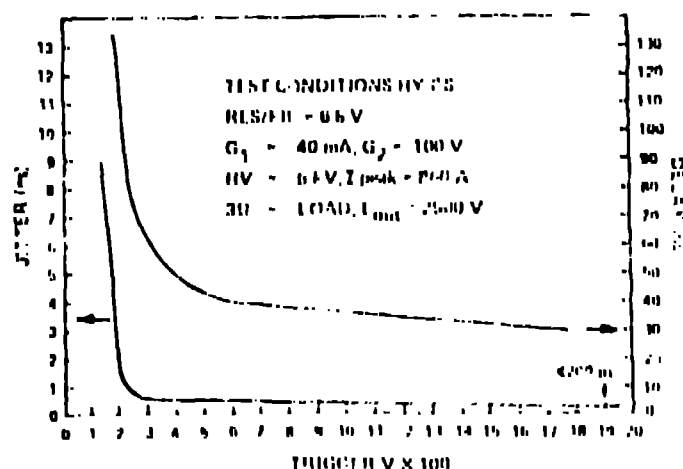


Fig. 25. Variation of delay (τ_d) and jitter (τ_j) times with peak grid trigger voltage for 1B6 Type HY-MS high-pressure triode hydrogen thyatron.

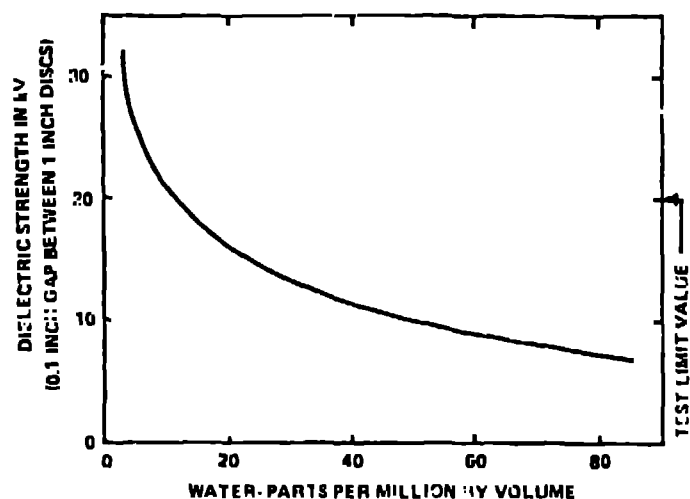


Fig. 26. High-voltage transformer oil dielectric strength as a function of water impurity concentration.

Several general suggestions in dc and low-frequency ac insulation are:(31)

- Design for 30,000 V peak per inch.
- Closer spacings require insulation barriers between high-voltage point and ground.
- Oil expansion with temperature is significant.
- Foreign matter can contaminate the oil (for example, wax-covered components, dirt, paint, etc.).
- Displace air in tanks with dry nitrogen or argon. (Freons can be used but absorb 10.6- μ m radiation.)
- Overstressing causes whirlpooling and can lead to internal arcs from particulate chaining.

Proper application of insulating materials is also an essential consideration in the design of high-voltage pulse transformers. At a minimum, it is necessary to know the effective dielectric strength of the materials and the voltage stresses that they will be subjected to in service. In reality, these two aspects are a complex of many factors, the details of which are beyond the scope of this paper.(8) It is useful, however, to summarize some of the general characteristics and modes of failure of dielectric materials.

For pulse transformers, the types of materials most commonly used are liquids and film or cast solids, usually in combinations. Failure in one invariably leads to failure in all. The initiating mechanism can be prompt in nature such as bulk breakdown, overstressing or gradual as a result of deterioration of dielectric strength from PDs. The process of dielectric deterioration from PDs primarily includes gas production in the liquids, which can lead to breakdown from gaseous inclusions and erosion of solids in contact with the liquids.

Three characteristics common to liquid and solid dielectrics used in pulsed voltage applications include:

ENERGY DISSIPATION IN THYRATRON (44122)

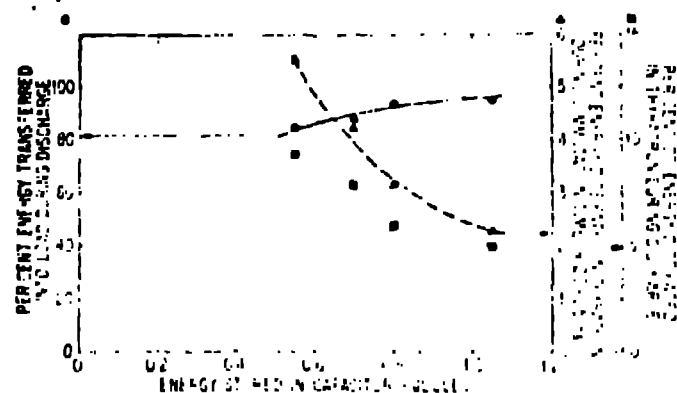


Fig. 22. Commutation and total discharge time energy loss for an FGAG low-inductance hydrogen thyatron as a function of energy stored in the capacitor. The peak current was 700 A and the pulse width 80 ns.

expected, so that low-loss switching is feasible with thyratrons, giving long economical life at high switching efficiencies. Retention of these low-energy losses remains to be confirmed at higher energy levels (>1 kJ).

New, compact, short-pulse thyratrons are currently under development for 50 to 150 kV multikilo-ohm operation at current rates of rise in excess of 10^{11} A/s at 10- to 100 kA peak-current levels. The newest 1-in. low-inductance thyatron currently under detailed study(21) is shown in Fig. 23 along with the recently developed T-4, Inc., integral current viewing resistor and di/dt monitor.

Table II tabulates salient features of present thyatron applications.(22)

The peak stand-off voltage vs pulse current for large commercial thyratrons shown in Fig. 24 is taken from T. R. Burkes' extensive switching report.(24)

Characteristics of developmental tetraode thyratrons are presented in Table III, clearly showing the major advances recently made in the field.

Switch Summary

Hydrogen thyratrons have many advantages when all things are considered. No other switch is yet capable of switching the same average power (1 MW) at the same efficiency (>90%) on a continuous basis.(25) High di/dt and pulse repetition-rate capabilities along with reasonably long life (2,000 to 10,000 h) make the thyatron invaluable in many applications wherein no other switch has all these demonstrated capabilities.(10) Even so, improvements in hydrogen thyratrons are continually being made.(27)

A further significant improvement could be made if a scheme can be found to better utilize the capabilities of the cathode. Such an improvement could lead to higher di/dt as well as peak current capabilities. An improvement in the emissivity of the cathode material would allow higher peak currents to be drawn. It has been many years since significant advances have been made in cathode capabilities.(28)

The capabilities of some switches have been greatly increased by the use of optical triggering tech-

niques, for example, laser-triggered spark gaps and silicon-controlled rectifiers. A similar technique may be applied to the thyatron. This technique might eliminate the effects (delay and jitter) incurred by the necessity of propagating a plasma and greatly increase the di/dt capability and cathode utilization of thyratrons.

Higher voltages in single-gap tubes have been achieved.(29) Current packaging techniques do not make use of this technology. Needs to date have emphasized low inductance and high average power more than voltage capability. The latter is now becoming an active research and development area.(27)

Numerous applications requiring very low jitters are arising. Recently, high pressure, low-inductance thyratrons have been developed(20) to meet multikilo-volt level nuclear particle diagnostic requirements for

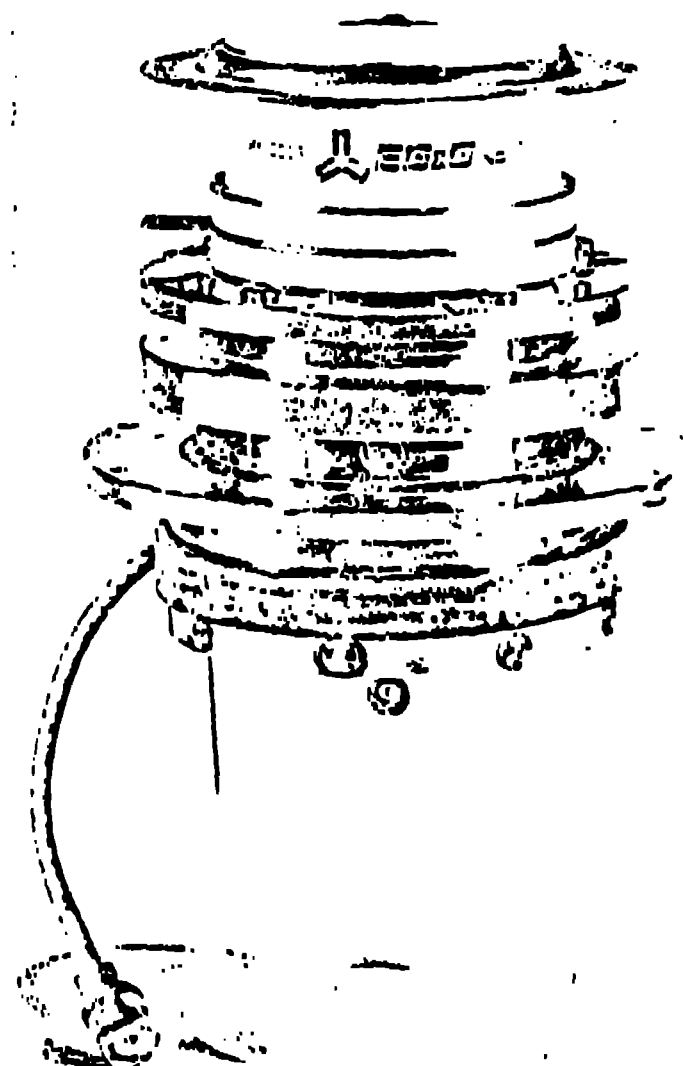


Fig. 23. Low-inductance thyatron with integral current viewing resistor and di/dt monitor.

TABLE IV

ONSET OF PARTIAL DISCHARGES IN VARIOUS OILS
TESTED IN LAMINATE STRUCTURES

	Dry Degassed Condition kV/cm	Barrel-Fresh Condition kV/cm
Mineral oil (inhibited)	325	250
X-ray oil (Marcel 2930)	590	510
Silicone oil (Dow Corning 200)	360	305
MIPB (Monsanto 1238)	620	410
DAA (HISOL SAS 101)	460	390
Paraffin oil (RTI-ep)	650	380

where

 V_0 is the total voltage across the electrodes, kV E_1 and E_2 are the voltage stresses in materials 1 and 2 ϵ_1 and ϵ_2 are the dielectric constants of materials 1 and 2 d_1 and d_2 are the thicknesses of materials 1 and 2.

Considerable caution must be exercised in interpreting dielectric strength and PD data because of differences in test conditions. Factors already mentioned such as pulse type, sample thickness, and area can yield results that differ by as much as an order of magnitude. This can be seen by comparing the CIV for silicone and mineral oil reported by Kuwahara et al., (37) with that obtained in the laminate tests. In the first case, measurements were made using close spaced needle-point electrodes with applied voltages between 15 and 20 kV. This resulted in a CIV of 3370 kV/cm for silicone oil and 3520 kV/cm for mineral oil. With the laminate, which were 1 cm thick and tested above 300 kV, the onset of PDs was observed at 360 kV/cm for silicone oil and 324 kV/cm for mineral oil with both oils in the dry degassed condition. These two sets of results emphasize the necessity of searching for data or conducting tests as near as possible to the actual service conditions that dielectrics will experience. Lacking such specific data, most common insulating liquids such as mineral oils, paraffin base oils, and silicone oils can be repetitively stressed to at least 150 kV/cm without encountering bulk breakdown or PD problems. If the oils are carefully filtered to remove particle matter larger than 1 μ m and are degassed before use, the margin of safety can be increased by at least 50%. When the highest possible performance must be obtained from an insulation system, there is no alternative to conducting tests as near as possible to anticipated service conditions.

CONCLUDING REMARKS

The emerging demands for high-reliability power conditioning components at multimegawatt power levels will require the continued research and development of new classes of low loss elements such as capacitors and switches. This overview paper has sought to present some of the technology base development under way in this country and to illustrate how different types of life-limiting effects start to come into play as pulse widths are shortened and repetition rates are increased. Multiyear lifetime components will demand the same or more research and development as was expended

in the past to create high-reliability components for radar modulator and aerospace applications.

REFERENCES

1. R. D. Guenther, J. L. May, and C. M. Stickley, "Items in Unclassified Particle Beam Research," Proc. Particle Beam Workshop, US Air Force Academy, Colorado Springs, Colorado, January 10-11, 1980.
2. G. McDuff, K. Rust, W. J. Sarjeant, and P. N. Mace, "Development of High Reliability, Multikilohertz Repetition-Rate Components," Proc. Fourteenth Pulse Power Modulator Symposium, Orlando, Florida, June 3-5, 1980, pp. 122-124.
3. G. McDuff, W. C. Nunnally, K. Rust, and W. J. Sarjeant, "Diagnostics and Performance Evaluation of Multikilohertz Capacitors," invited paper to be published in the Proc. Special Symposium on High Energy Density Capacitors and Dielectric Materials at the 1980 National Academy of Sciences Conference on Electrical Insulation and Dielectric Phenomena, Boston, Massachusetts, October 26-28, 1980.
4. G. I. Frense, C. G. Dalton, and W. J. Sarjeant, "Repetitive Megamp per Microsecond di/dt Pulsers for Driving Sub-ohm Transmission Line Neutrino Particle Detectors," Proc. Fourteenth Pulse Power Modulator Symposium, Orlando, Florida, June 3-5, 1980, pp. 161-163.
5. G. H. Mauldin, "The Application of Perfluorocarbons as Impregnants for Plastic Film Capacitors," to be published in the Proc. of the NASA Symposium, Huntsville, Alabama, February 14, 1981.
6. G. H. Mauldin, "The High Energy Density Capacitor Program at Sandia National Laboratories," invited paper to be published in the Proc. of the Special Symposium on High Energy Density Capacitors and Dielectric Materials at the 1980 National Academy of Sciences Conference on Electrical Insulation and Dielectric Phenomena, Boston, Massachusetts, October 26-28, 1980.
7. "Capacitors for Aircraft High Power," Air Force Aero Propulsion Laboratory, Air Force Systems Command technical report AFAPL-TR-75-19, February 1975.
8. "High Voltage Design Guide for Airborne Equipment," Boeing Aerospace Corp. technical report AB 4079-269, June 1976.
9. T. R. Burkes and W. J. Sarjeant, "Electromechanical Shock in Pulse Power Components," Proc. Fourteenth Pulse Power Modulator Symposium, Orlando, Florida, June 3-5, 1980, pp. 125-129.
10. G. P. Holcourt, "Capacitor Development for SCVFIAC," Symposium on Engineering Problems of Fusion Research, Los Alamos National Laboratory, Los Alamos, New Mexico, April 8-11, 1969, paper CI 2.
11. G. P. Holcourt, "Problems in the Design and Manufacture of Energy Storage Capacitors," Los Alamos National Laboratory report LA 4141-MS, January 1970.

12. "Development of a High Energy Density Capacitor for Plasma Thrusters," Air Force Rocket Propulsion Laboratory, Air Force Systems Command technical report AFRPL-TN-80-35, October 1980.
13. J. Power, W. Nunnally, and D. Young, "A 100-kV, 2-ns Rise-time, dc-Coupled Probe," Workshop on Electrical Measurements in Pulse Power Systems, National Bureau of Standards, Boulder, Colorado, March 2-4, 1981.
14. W. J. Sarjeant, "Energy Storage Capacitors," submitted for publication in the Proc. IEEE Plasma Science Pulse Power Course, Santa Fe, New Mexico, May 18-22, 1981.
15. Executive Summary to the National Academy of Sciences, Special Symposium on High Energy Density Capacitors and Dielectric Materials at the 1980 Conference on Electrical Insulation and Dielectric Phenomena, Boston, Massachusetts, October 26-28, 1980.
16. "Technical Development of High Energy Density Capacitors," NASA report CR14926, February 1976.
17. T. H. Martin, "FRIZZ--A High Voltage Impulse Tester," Sandia National Laboratories report SC-RR-71, 0341, June 1971.
18. G. J. Rohwein, "Design of Pulse Transformers for PFI Charging," Proc. 2nd IEEE International Pulsed Power Conference, Lubbock, Texas, June 1979.
19. Y. Finkelstein, P. Goldberg, and J. Shuchatowitz, "High Voltage Impulse System," Rev. Sci. Instr., Vol. 37, No. 2, February 1962.
20. J. C. Martin, P. D. Champney, and D. H. Hammer, "Notes on the Construction Methods of a Martin High Voltage Pulse Transformer," School of Electrical Engineering, Cornell University, June 1967.
21. G. J. Rohwein, "A 3 MV Transformer for PFI Pulse Charging," IEEE Trans. on Nucl. Sci., Vol. NS 26, No. 3, June 1979.
22. M. T. Buttram and G. J. Rohwein, "Operation of a 300 kV, 100 Hz, 30 kW Average Power Pulsar," Proc. 13th Pulsed Power Modulator Symposium, Buffalo, New York, June 1978.
23. EG&G technical literature.
24. T. R. Burkes, "A Critical Analysis and Assessment of High Power Switches," Naval Surface Weapons Center report N930/78, September 1978.
25. J. J. Hamilton, S. Mertz, R. Plante, D. Turnquist, N. Reinhardt, J. Creedon, and J. McGowan, "Development of a Forty Kilovolt Megawatt Average Power Thyatron (MAPS-40)," Proc. 13th Pulse Power Modulator Symposium, Buffalo, New York, June 1978.
26. S. Friedman, S. Goldberg, J. Hamilton, S. Mertz, R. Plante, and D. Turnquist, "Multigigawatt Hydrogen Thyatrons with Nanosecond Rise Times," Proc. 13th Pulse Power Modulator Symposium, Buffalo, New York, June 1978.
27. D. Turnquist, R. Caristi, S. Friedman, S. Mertz, R. Mautsch, and N. Reinhardt, "New Hydrogen Thyatrons for Advanced High Power Switching," Proc. 2nd IEEE International Pulsed Power Conference, June 12-14, 1979.
28. R. L. Remski, "1978 Tri-Service Cathode Workshop," Microwave J., Vol. 21, No. 7, July 1978.
29. L. Mancebo, "A High Power Hydrogen Thyatron Without Gradient Grids," Proc. 10th Modulator Symposium, May 1968.
30. G. Krausse and W. J. Sarjeant, "Sub-Nanosecond Jitter, Repetitive Impulse Generators for High Reliability Applications," to be presented at the IEEE International Pulsed Power Conference, Albuquerque, New Mexico, June 1981.
31. W. J. Sarjeant, "DC Power Supplies and Hard-Tube Power Conditioning Systems," submitted for publication in the Proc. IEEE Plasma Science Pulse Power Course, Santa Fe, New Mexico, May 18-22, 1981.
32. K. C. Kao and J. P. C. McMath, "Time-Dependent Pressure Effect in Liquid Dielectrics," IEEE Trans. on Elec. Insulation, Vol. EI-5, No. 3, September 1970.
33. F. Tse, W. Hell, M. Mulcahy, and P. Holin, "Liquid Insulation," High Voltage Technical Seminar, Ion Physics Corp., Boston, Massachusetts, September 1969.
34. G. J. Rohwein, Unpublished Oil Breakdown Data, Sandia National Laboratories, Albuquerque, New Mexico, January 1980.
35. F. M. Clark, Insulating Materials for Design and Engineering Practice, (J. Wiley and Sons, Inc., New York, London) 1962.
36. G. J. Rohwein, Unpublished Results of Oil-Laminate Tests, Sandia National Laboratories, Albuquerque, New Mexico, 1979.
37. H. Kuwahara, K. Tsuruta, H. Munemura, T. Ishii, and H. Shiomi, "Partial Discharge Characteristics of Silicone Liquids," Trans. IEEE Power Engineering Society, January 1975.